On elongated gas pockets in downward sloping pipelines

I.W.M. Pothof[1,2]*, F.H.L.R. Clemens[2]

[1] *Deltares | Delft Hydraulics, Department of Industrial Hydrodynamics, P.O. Box 177, 2600 MH Delft, The Netherlands.*
[2] *Sanitary Engineering Group, Department of Civil Engineering and Geosciences, Delft University of Technology, P.O. Box 5, 2600 AA Delft.*

**Corresponding author, e-mail ivo.pothof@deltares.nl*

ABSTRACT

This paper investigates the behaviour of elongated gas pockets in downward sloping pipes. It provides a description of the relevant physical processes, supported by literature and recently performed experiments in different test rigs, operated by Deltares | Delft Hydraulics. Two criteria are derived from energy considerations. These criteria define a confined range of velocities, in which balanced elongated pockets will occur. This velocity range for balanced gas pockets is a function of the downward slope. Furthermore, a momentum balance is derived that predicts the clearing velocity of elongated gas pockets as a function of the downward slope. All analytical considerations are substantiated with experimental data.

KEYWORDS

Gas bubbles; pipelines; gas transport; two-phase flow; plug flow; surface tension, hydraulic jump.

1. INTRODUCTION

Water pipelines and wastewater pressure mains in particular are subject to gas pockets in declining sections. These gas pockets cause an additional head loss and an associated capacity reduction. Gas pockets in pressurised wastewater mains generally cannot be expelled with air valves for various reasons:

- hazardous gases may be released,
- many air valves do not cope appropriately with the composition of wastewater and remain closed or, even worse, remain open after the air has been expelled, and/or
- the preferred air valve location is on private property or on an inaccessible location for maintenance.

The gas pocket head loss is approximately equal to the height of the gas pocket, which causes a inacceptable capacity reduction in transportation pipelines in urbanised delta areas, which were designed with a negligible static head. The clearing velocity, i.e. the velocity to clear gas pockets from a downward slope or to remove the additional gas pocket head loss, cannot be predicted with sufficient accuracy, since existing experimental correlations show opposing trends at certain downward slopes.

Despite its practical relevance the breakdown and transport of gas pockets in downward sloping liquid pipes has not been studied on a continuous basis. The available literature includes less than 10 investigations on gas transport in downward slopes by hydraulic means.

A wide spread in experimental correlations on the clearing velocity and downward slope has been reported by various authors; see e.g. (Escarameia 2006).

The elongated bubble velocity in horizontal and upward inclining pipes has been investigated more intensively, because of its relevance for flow regime transitions in two- and multiphase flows with typical applications in the oil and gas industry (Zukoski 1966; Bendiksen 1984). The existing numerical two-phase flow models encounter various difficulties in downward sloping pipes, which are related to the typical physical phenomena in downward slopes (Taitel, Sarica et al. 2000).

The main objective of this paper is a contribution to the modelling of the transport phenomena that dominate the break down and transport of elongated gas pockets in downward sloping pipes for liquid transport.

Section 2 summarises the physical processes that determine the transport of gas pockets in downward slopes. Section 3 summarises the literature on the behaviour of gas pockets in downward slopes. The range of liquid velocities that enable balanced gas pockets is derived from energy considerations in Section 4. Section 5 derives the applicable momentum balance for the clearing of gas pockets from downward slopes. Section 6 shows that an alternative dimensionless velocity is a more appropriate scaling parameter for pipes, smaller than 200 mm. Conclusions and recommendations for further research are listed in sections 7 and 8.

Terminology

Since the literature on elongated bubbles stems from both petroleum engineering and civil engineering, the key notions are summarised hereafter:

- The *clearing velocity* is defined as the required liquid velocity to transport a gas bubble to the bottom of a downward slope.
- The *drift velocity* is defined as the gas bubble velocity in a stagnant liquid. The civil engineering equivalent of the drift velocity is the rise velocity or bubble rise velocity.
- The *bubble velocity* is defined as the actual bubble velocity in a flowing liquid. The bubble velocity is generally modelled as a linear combination of the superficial liquid velocity and the drift velocity.
- The *(liquid) film velocity* is the actual liquid velocity underneath a gas pocket.
- A gas pocket or plug is defined *stable*, if no smaller bubbles are ejected from the bubble by the surrounding liquid. The gas pocket is not large enough to generate a gas entraining hydraulic jump.
- An elongated bubble is defined *balanced*, if the bubble stays balanced in the downward slope with zero bubble velocity.
- the *superficial velocity* is the average phasic velocity at a full pipe cross section.
- The *dimensionless gas pocket volume* is the gas pocket volume in terms of a cylinder length expressed in pipe diameters.
- The Froude scaled dimensionless velocity, known as the *flow number*, is defined as

$$F = \frac{v_{sl}}{\sqrt{gD}} \tag{1}$$

where v_{sl} is the superficial liquid velocity. The flow number should not be confused with the Froude number, which is defined as the ratio of the actual liquid film velocity and shallow water wave propagation speed:

$$Fr = \frac{v_l}{\sqrt{g \frac{A_l}{T_l}}} \tag{2}$$

where subscript l refers to an arbitrary location underneath an elongated gas bubble, v_l refers to the liquid film velocity and T_l is the local surface width. The ratio A_l / T_l is known as the hydraulic depth or effective depth, y_e.

2. PHYSICAL PROCESSES

This section discusses the physical processes of downward co-current air-water flow at very small superficial gas velocities (order of 1 mm/s) and moderate superficial liquid velocities (order of 1 m/s). The description of the physical processes stems from visual observations in various transparent test rigs at Deltares | Delft Hydraulics (Lubbers and Clemens 2005; Lubbers and Clemens 2006), (Tukker 2007) and (Stegeman 2008) and from available literature.

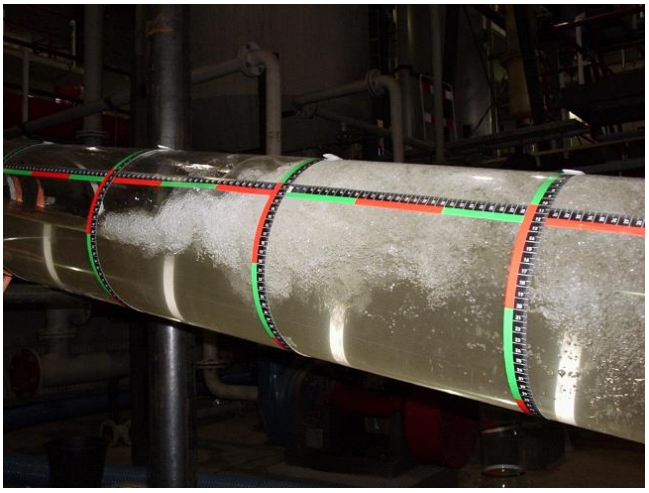

Figure 1. Gas entrainment in the hydraulic jump

If an air pocket is present in the top of a declining section and a liquid is flowing through the conduit, then the water flow accelerates underneath the gas volume and tends towards the normal flow condition. At the end of the gas volume a hydraulic jump is present that entrains air into the flowing water; this process is referred to as *the pumping action of the hydraulic jump* (Figure 1). The suspended bubbles have a tendency to coalesce and rise towards the pipe soffit in the aeration zone. The gas plugs along the pipe soffit may return to the gas pocket in the top, may stay static in one position and grow to new elongated pockets with a hydraulic jump or may steadily move downward; these situations depend on the superficial water velocity. Kalinske and Bliss were one of the first to describe these flow regimes (Kalinske 1943):

- A blow-back flow regime at relatively small discharges. In this flow regime, the bubbles coalesce and periodically blow back upward, which limits the net gas transport. The net gas transport is controlled by the flow characteristics below the hydraulic jump, which are described by the flow number; see eq. (1).
- A full gas transport flow regime at higher discharges, at which all entrained gas bubbles are transported to the bottom of the downward slope. The gas transport becomes almost independent of the flow number in this flow regime. Kalinske et al.

(1943) conclude that the Froude number (eq. (2)) upstream of the hydraulic jump determines the gas transport.

- At the transition from the blow-back flow regime to the full gas transport flow regime, a series of two to four balanced gas pockets and hydraulic jumps were observed in the downward slope. The length of the downward slope of their test rig was 10.5 m long with internal pipe diameter of 100 mm and 149 mm (0.49 ft). Blow-back did not occur any more in this transitional flow regime.

It is clear from Kalinske's observations that the maximum flow number with balanced gas pockets is equivalent with the clearing flow number. The number of consecutive hydraulic jumps depends on the downward slope, the liquid velocity and the length of the slope. The additional head loss by the gas pocket gradually diminishes as the water velocity increases. If the additional head loss has just diminished, then the gas is flowing downward in stable plugs at a smaller velocity than the liquid velocity.
If the downward slope is long enough and the liquid velocity is within a certain range, then several consecutive balanced elongated bubbles and hydraulic jumps are present in the downward slope (Bliss 1942; Kent 1952; Stegeman 2008).

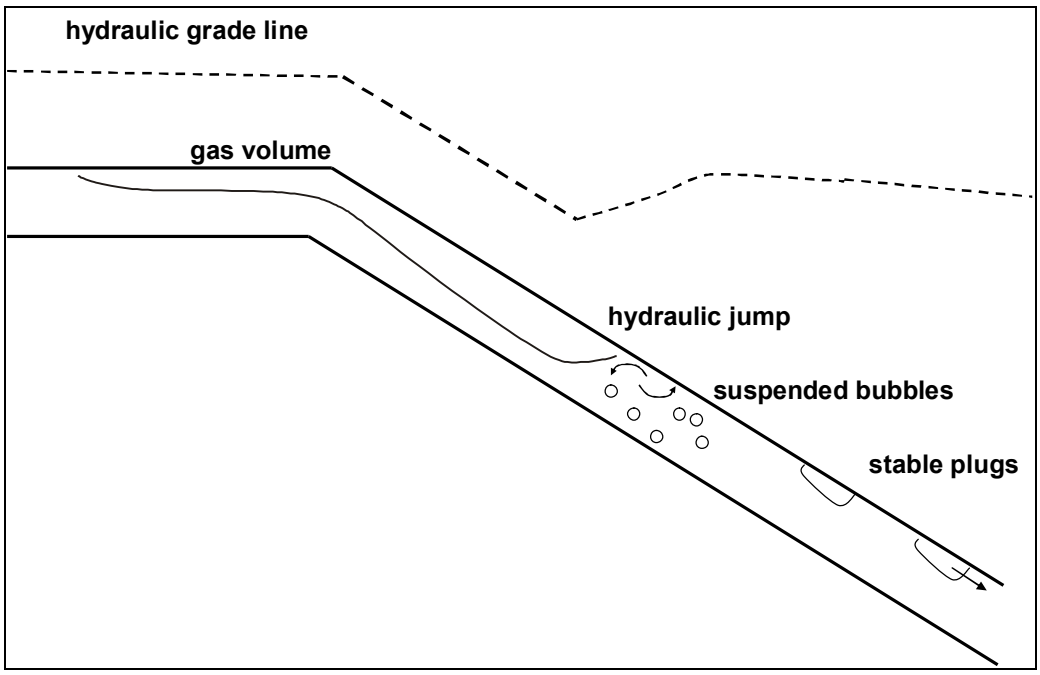

Figure 2. Schematic overview of downward gas transport by flowing water near the clearing velocity.

The aforementioned description of the physical processes triggers more detailed investigations into the motion of elongated gas bubbles.

3. LITERATURE ON ELONGATED GAS BUBBLES

This section details the behaviour of elongated gas bubbles and investigates the applicable momentum and energy balances that explain the observed phenomena. We have reviewed the available literature on elongated gas bubbles (Pothof 2008); this conference paper has been

invited for journal publication (Pothof 2009 (in review)). The main conclusions from this literature review are briefly summarised hereafter.

First, Pothof et al. (Pothof 2008) have shown that the reported wide spread in available experimental correlations on clearing velocity as a function of downward slope is mainly caused by misquoting certain references, human errors and wrongful comparison of different processes. Wisner et al. (Wisner, Mohsen et al. 1975) have misquoted Kalinske and Bliss in equation (3) by using a coefficient 0.707 instead of the correct coefficient 1/0.71, which (incorrectly) resulted in 30% smaller flow numbers. Furthermore, Kalinske and Bliss' equation is an equation for the initiation of gas transport, although it has been referenced as an equation for the clearing velocity. Kalinske and Bliss: "...to maintain proper air removal, the actual value of the water discharge should be appreciably larger than Q_i" (Kalinske 1943).

$$F_i = \frac{4}{\pi}\sqrt{\frac{\sin\theta}{0.71}} \approx 1.5\sqrt{\sin\theta} \tag{3}$$

The transition to full pipe flow occurs at flow numbers between 0.7 and 1 at slopes smaller than 8°; see Figure 4. Kent (1952) has produced an interesting PhD thesis on the entrainment of air by flowing water in downward slopes, from which no journal publications have been extracted for unknown reasons. Kent focused on the transitional flow regime with stable gas pockets and established the following correlation between the clearing flow number and pipe slope from his experiments:

$$\frac{v_{sl,c}}{\sqrt{gD}} = 1.23\sqrt{\sin\theta} \tag{4}$$

Unfortunately, Kent made a human error in his data analysis, which is illustrated in Figure 3; equation (4) should be a straight line through the origin in Figure 3.

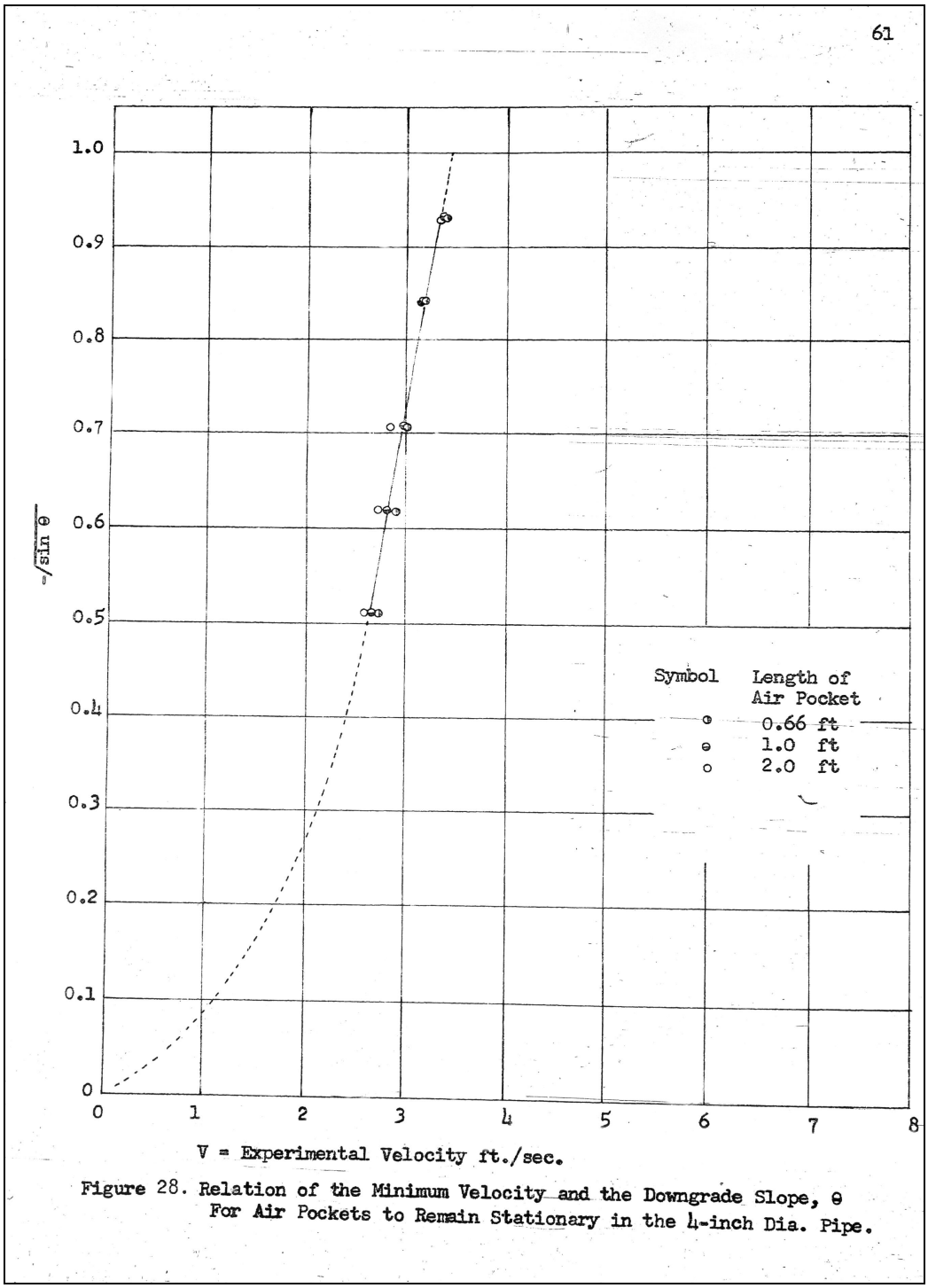

Figure 3. Kent's erroneous curve fit

A better curve fit on Kent's data, which allows for a non-zero offset is given in equation (5); see (Mosvell 1976), (Lauchlan 2005) and (Wisner, Mohsen et al. 1975), who first published the systematic deviation between Kent's data and equation (4).

$$\frac{v_{sl,c}}{\sqrt{gD}} = 0.55 + 0.5\sqrt{\sin\theta} \tag{5}$$

Finally, the existing literature includes two different approaches on establishing the clearing velocity. One approach, adopted by Bliss (1942) and Lubbers (Lubbers 2007a; Lubbers 2007b), is based on the injection of air upstream of the downward slope. Most other investigators inject air directly in the slope (Kent 1952; Gandenberger 1957; Wisner, Mohsen et al. 1975; Escarameia 2006). One disadvantage of the second approach is that the gas pocket can be forced to a certain size, that could not occur if the gas pocket was introduced upstream of the slope. This implies that comparing both approaches has its limitations.

The existing literature on gas transport in downward slopes can be extended with literature on upward bubble drift velocities for two reasons. First, some investigators have extended their experiments to downward slopes (Zukoski 1966; Bendiksen 1992). Second, the bubble drift velocity at +90° is strongly related to the clearing velocity at –90°. At intermediate slopes the clearing velocity is greater than the drift velocity; Gandenberger (1957) has measured clearing velocities that are 30% to 60% greater than the drift velocity in a 45 mm diameter pipe.

Bendiksen injected air bubbles in the sloping section of a 24.2 mm pipe at angles from -30° to +90°. Bendiksen's drift velocity model can be extended to downward slopes by just multiplying the horizontal drift component with the sign of the pipe angle, yielding:

$$\frac{v_{sl,d}}{\sqrt{gD}} = 0.34\sin\beta + 0.54\,\mathrm{sgn}\left(\beta\right)\cdot\cos\beta \tag{6}$$

Equation (6) implies that the drift velocity tends to -0.54 for small downward slopes and to +0.54 for small positive slopes. A physical explanation for this transition has been given by Benjamin (1968) and Montes (1997). Combining equation (6) with Bendiksen's equation for the bubble velocity yields an expression for the stable gas pocket flow number at downward slopes.

$$F_c = \frac{v_{sl,c}}{\sqrt{gD}} = \frac{-v_{sl,d}}{C_0\sqrt{gD}} \tag{7}$$

where Bendiksen mentions a slip parameter C_0 equal to 0.98 for downward slopes (up to 30°). This value of the slip parameter is valid for flow numbers up to 3.5. It is assumed that the same slip parameter is applicable to all downward slopes. Bendiksen's coefficient 0.34 for vertical pipes stems from detailed experiments on drift velocities by Zukoski (1966). Zukoski's data on elongated bubble rise velocities shows that the bubble rise velocity scales with $\sqrt{gD}$, Zukoski's data shows that the bubble rise flow number at 90° remains constant (0.34), if the Eötvös number is greater than 40; at other slopes the drift flow number continues to increase up to a Eötvös number of at least 4000. Zukoski's and Bendiksen's results are intercomparable. Lubbers' measurements at a downward slope of 90° confirms that a flow number of 0.4 is sufficient to transport gas pockets in downward direction (Lubbers 2007).

Lubbers has performed experiments in three different pipe sizes (110 mm, 220 mm and 500 mm) at various downward slopes from 5° to 30° and 90° (Lubbers 2007a; Lubbers 2007b). Lubbers injected air continuously upstream of the downward slope in the horizontal section and determined the extra head loss due to the gas volume at different combinations of air and liquid flow rate. The clearing flow number is reached when the extra head loss due to the presence of the gas flow attains a minimum. This minimum value is close to zero. Lubbers found that the largest clearing flow number is required at downward slopes of approximately 10°. Figure 4 shows a gradual drop in clearing flow number at slopes above 10°. The clearing flow number drops to about 0.4 for a vertical pipe with 220 mm internal diameter. An

intercomparison of the clearing flow numbers at a downward slope of 10° and the three pipe sizes, revealed that the clearing velocity at 110 mm was smaller than at 220 mm or 500 mm. Therefore, Tukker (2007) has extended these tests to pipe diameters of 80 mm and 150 mm at the same downward slope of 10°. The length of the downward slope in the aforementioned investigations was 30D, although Lubbers acquired a data set with a longer downward slope of 57D and 20°. Tukker and Stegeman have described the flow regimes in addition to the automated data acquisition. Lubbers has described the flow regimes for his 110 mm and 220 mm experiments.

Montes (1997) has provided a more fundamental basis for the formation of elongated cavities in horizontal pipes with a free outflow. Montes' analysis is based on a specific energy criterion, taking into account that the bubble nose is a stagnation point, as already pointed out by Benjamin (1968). The stagnation criteria for rectangular and circular conduits yield:

Rectangular:
$$\begin{cases} y_{cr} + \dfrac{v_{cr}^2}{2g} = \dfrac{3}{2} y_{cr} = D \\ F_s = \left(\dfrac{2}{3}\right)^{1.5} = 0.5443 \quad at \quad \dfrac{y_{cr}}{D} = \dfrac{2}{3} \end{cases} \tag{8}$$

Circular:
$$\begin{cases} y_{cr} + \dfrac{v_{cr}^2}{2g} = y_{cr} + \dfrac{A_{cr}}{2T_{cr}} = D \\ F_s = 0.5818 \quad at \quad \dfrac{y_{cr}}{D} = 0.6886 \end{cases} \tag{9}$$

where the subscript *cr* refers to critical free surface flow, at which the convectional velocity equals the shallow water wave speed. Montes' criteria must be interpreted as follows. If the flow number is smaller than the stagnation flow number, then the cavity will extend in upstream direction and a free surface channel flow profile is present in the horizontal section. If the flow number is greater than the stagnation flow number, then a considerably shorter cavity will be present at the outflow. A second criterion, developed by Montes, is the transition to full pipe flow, which occurs at $F_p = 1$. This criterion is based on the fact that small negative free surface waves travel at a velocity of $\sqrt{gD}$. Montes incorrectly claims that the full pipe flow criterion applies to both rectangular and circular conduits, but the continuity equation in appendix II (Montes 1997) is valid for rectangular conduits only. A derivation of the full pipe flow criterion for any cross section is as follows, considering a infinitesimal negative wave travelling with absolute velocity *c*:

Continuity:
$$\left(c + v_{sl}\right) A = \left(c + v_{sl} + \delta v\right)\left(A - \delta A\right) \tag{10}$$

Energy:
$$D + \frac{\left(c + v_{sl}\right)^2}{2g} = D - \delta y + \frac{\left(c + v_{sl} + \delta v\right)^2}{2g} \tag{11}$$

Elimination of the velocity increment δv, recognising that $\delta A / \delta y = T$, yields:

$$\left(c + v_{sl}\right) = \pm\sqrt{\frac{gA}{T}} \tag{12}$$

At the full pipe flow condition the wave is balanced, hence $c = 0$, and the full pipe flow criterion for an arbitrary conduit cross section becomes:

$$F_p = \frac{v_{sl}}{\sqrt{gD}} = \sqrt{\frac{A}{TD}} \tag{13}$$

The above criterion reduces to $F_p = 1$ for rectangular conduits, but tends towards infinity in a circular conduit. Consequently, the full pipe flow criterion is not applicable in circular conduits. Hager, Montes and others have shown experimentally that the transition to full pipe flow in a horizontal pipe occurs at a flow number of 1.15 in large diameter pipes (Montes 1997; Hager 1999).

4. ENERGY CONSIDERATIONS

Montes' stagnation criterion can be generalised to arbitrary slopes.

$$y_s \cos\theta + \frac{v_l^2}{2g} = D\cos\theta \quad \Leftrightarrow \quad y_s \cos\theta + \frac{v_{sl}^2}{2g}\left(\frac{A}{A_s}\right)^2 = D\cos\theta \tag{14}$$

$$F_s = \left(\frac{A_s}{A}\right)\sqrt{2\left(1-\frac{y_s}{D}\right)\cos\theta} \le 0.5818\sqrt{\cos\theta} \tag{15}$$

The stagnation criterion attains a maximum value at a local Froude number of unity for all pipe slopes, which coincides with the critical depth of 0.6886D. This criterion must be interpreted as a minimum flow number for elongated bubble stabilisation. If the flow number is smaller than the stagnation flow number, F_s, the elongated bubble will move upward.

The full pipe flow criterion at arbitrary pipe slopes is assumed to follow a similar profile although experimental evidence is lacking at this moment.

$$F_p = 1.15\sqrt{\cos\theta} \tag{16}$$

The full pipe flow criterion represents the maximum flow number at which stable elongated bubbles can occur. If the flow number exceeds the full pipe flow number, F_p , then all elongated bubbles will be pushed in downward direction. Hence balanced gas pockets can occur only if the flow number is within the range between the stagnation flow number, F_s , and the full pipe flow number, F_p. These criteria are based on gravity driven flow considerations and are not applicable at very steep slopes; Zukoski's measurements should prevail at very steep pipe slopes. The data from Bliss and Lubbers are well within the proposed range.

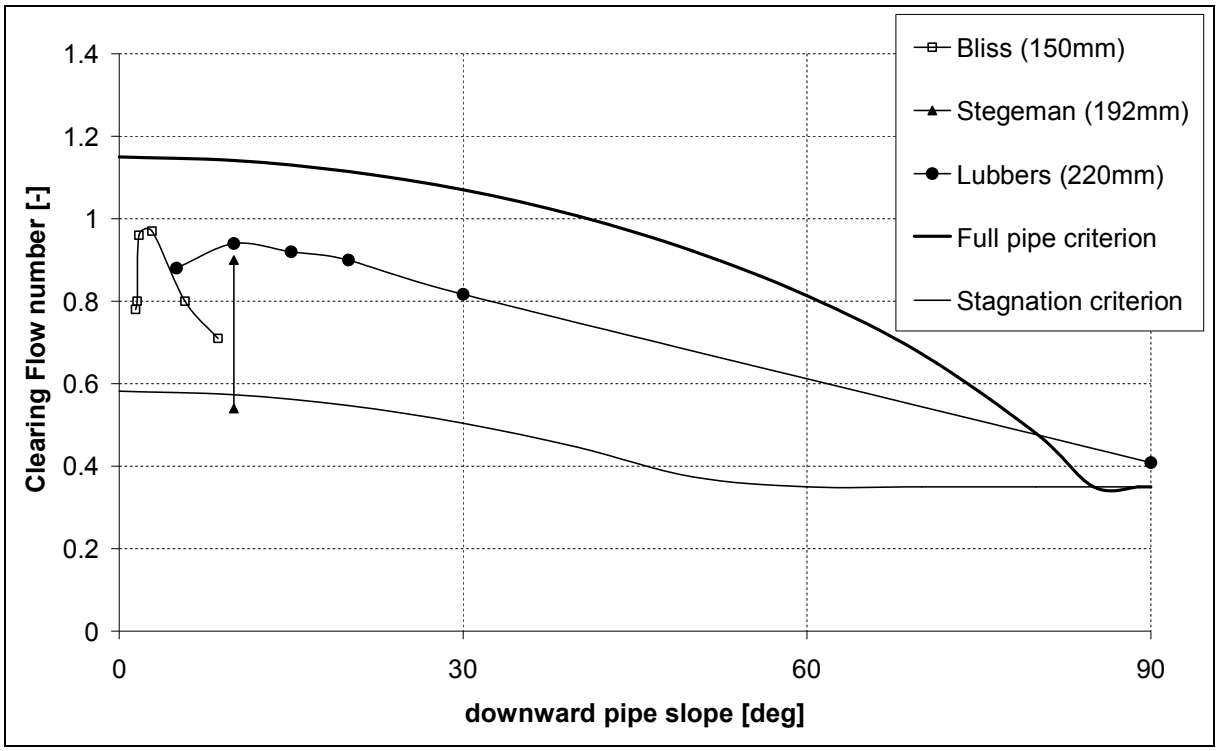

Figure 4. Clearing flow numbers from Bliss, Lubbers and Stegeman

Figure 5 shows experimental correlations between the pipe slope and the balancing velocity of elongated bubbles from various authors that have injected gas pockets in the sloping section. A comparison of these measurements shows that the clearing velocity increases with diameter. It is noted that most of the data fits within the two proposed criteria. Kent's data on the 60° slope was possibly affected by the presence of the gas injection point.

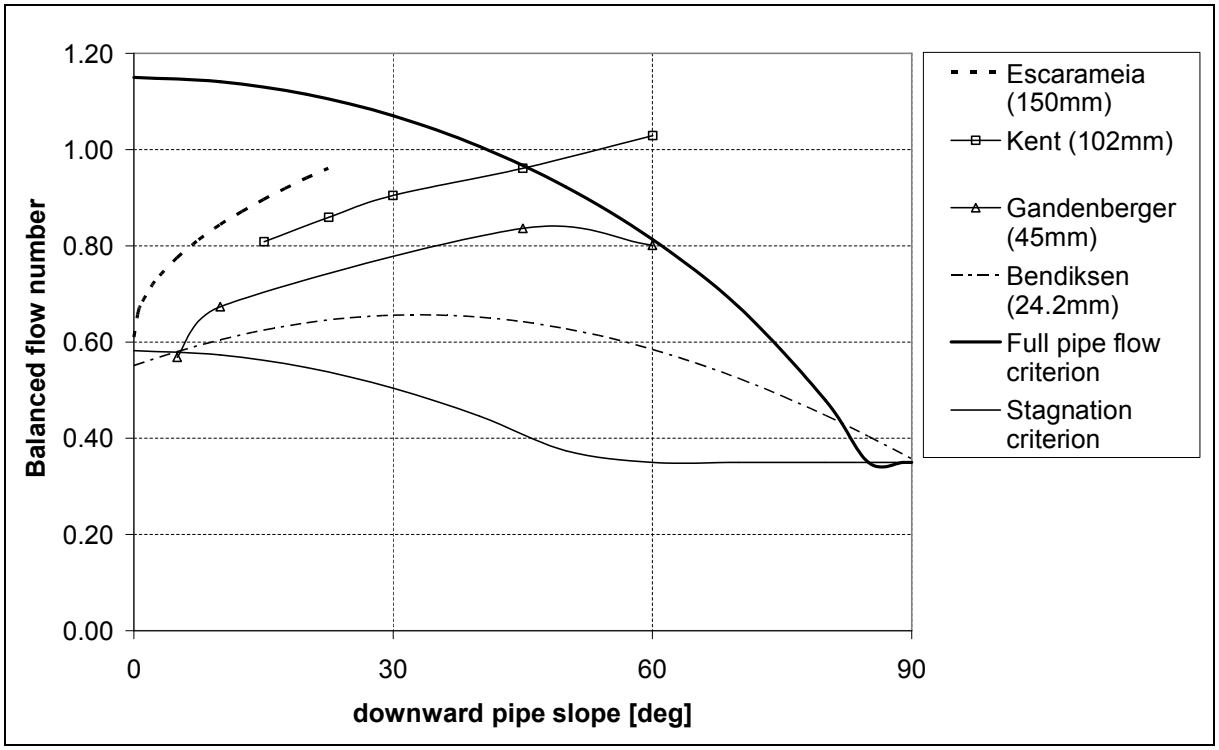

Figure 5. Flow number correlations and energy criteria for balanced gas pocket presence

5. MOMENTUM CONSIDERATIONS

The energy considerations, discussed above, provide necessary conditions on the flow number for the existence of balanced elongated gas pockets in a downward slope. This section investigates the applicable momentum balance on an elongated gas pocket. The gas pocket motion is defined by the forces on the dashed control volume, sketched in Figure 6.

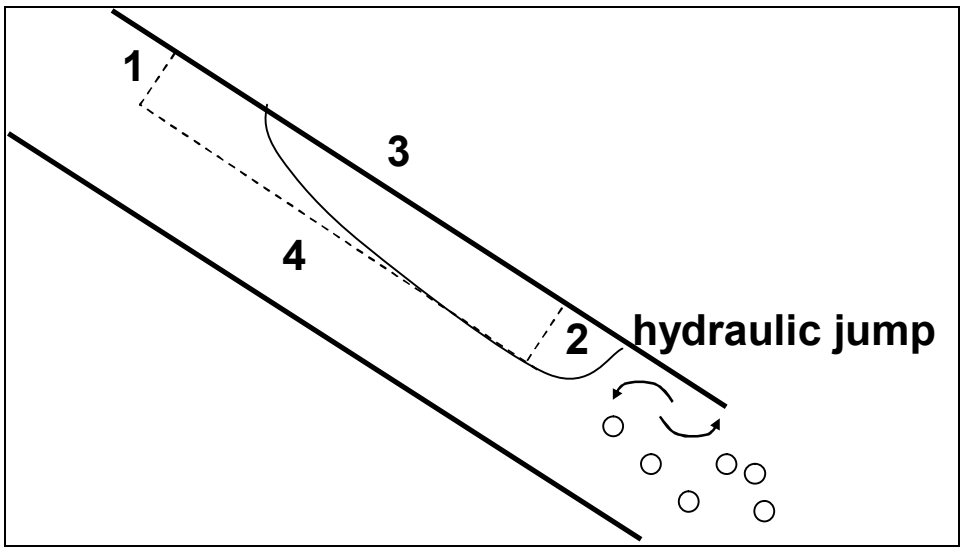

Figure 6. Definition sketch for momentum balance on elongated gas pocket

The force on surface "2" is equal to the gas pocket pressure, p_g , multiplied by the gas pocket area A_b at the hydraulic jump. The liquid pressure at the stagnation point at the nose of the gas pocket equals the gas pocket pressure, recognising that surface tension effects due to interface curvature can be safely neglected. The upstream boundary of the control volume, location "1", is sketched some distance upstream of the gas pocket nose where the liquid streamlines are parallel. The local pressure at the pipe soffit is smaller than the gas pocket pressure for two reasons: first, the larger elevation, second, the liquid streamlines decelerate towards the stagnation point at the bubble nose, according to Bernoulli. The exact distance from boundary "1" to the bubble nose, denoted by X, will be proven to be eliminated from the momentum balance; nevertheless, this distance is assessed to be in the order of the bubble height.

$$p_1(y=D) = p_g - \frac{\rho}{2} v_{sl}^2 - \rho g \cdot X \cdot \sin\theta \tag{17}$$

Since the liquid streamlines are parallel at boundary "1", the liquid pressure is hydrostatic. Hence the average surface pressure on boundary "1" is obtained after integration of the hydrostatic pressure across the bubble surface area.

$$p_1 = p_g - \frac{\rho}{2} v_{sl}^2 - \rho g \cdot X \cdot \sin\theta + \cos\theta \cdot \frac{\rho g}{A_b} \int_{y_b}^{D} (D-y)\, w(y)\, dy \tag{18}$$

The integral term can be solved analytically resulting in:

$$\int_{y_b}^{D} (D-y)\, w(y)\, dy = R^3 \left[\frac{2}{3} \sqrt{\frac{2y_b}{R} - \left(\frac{y_b}{R}\right)^2} \left(\frac{y_b}{R} - 3\right) \left(\frac{y_b}{R} - \frac{1}{2}\right) + \arcsin\left(1 - \frac{y_b}{R}\right) + \frac{\pi}{2} \right] \tag{19}$$

The body force on the control volume includes the liquid mass between boundary "1" and the bubble nose; the mass of the gas pocket is neglected. No shear force acts on the control

volume along the pipe soffit (boundary "3"), because the gas pocket is not moving; even if the gas pocket would move at a constant speed, this shear force can still safely be neglected, because of the large liquid gas density ratio.

The axial liquid momentum, entering at boundary "1", increases in the control volume and leaves at boundary "4". This momentum increase is caused by the shear force, exerted by the liquid motion underneath the gas pocket on boundary "4". Consequently, these two momentum terms are cancelled by the liquid shear on boundary "4". A physical explanation is that the elongated gas pocket motion is not affected by the liquid acceleration around the bubble nose. This observation, or assumption, simplifies the momentum balance to a sum of pressure forces on boundary "1" and "2" and a body force.

$$p_1 \cdot A_b - p_g \cdot A_b + A_b \cdot X \cdot \rho g \cdot \sin\theta = 0 \tag{20}$$

A further simplification eliminates the gas pressure and the distance X, such that division by $A_b \cdot \rho \cdot g \cdot D$ results in a non-dimensionalised pressure balance.

$$\frac{v_{sl}^2}{gD} = \frac{A}{A_b}\frac{\cos\theta}{\pi}\left[\frac{2}{3}\sqrt{\frac{2y_b}{R} - \left(\frac{y_b}{R}\right)^2}\left(\frac{y_b}{R} - 3\right)\left(\frac{y_b}{R} - \frac{1}{2}\right) + \arcsin\left(1 - \frac{y_b}{R}\right) + \frac{\pi}{2}\right] \tag{21}$$

This resulting momentum balance states that a gas pocket is moving at a constant velocity (including 0 velocity) if the stagnation pressure equals the average hydrostatic pressure upstream of the gas pocket. It is believed that this momentum balance is applicable for all situations in which the liquid film is supercritical and generates a hydraulic jump behind the gas pocket. The maximum gas pocket area coincides with a liquid film at normal depth at the hydraulic jump. Equation (22) shows the normal depth equation in a non-dimensional format.

$$\frac{v_{sl}^2}{gD} = \frac{2\sin\theta}{\lambda}\frac{D_h}{D}\left(\frac{A_n}{A}\right)^2 \tag{22}$$

The friction factor, λ, can be computed from the White-Colebrook equation. Equations (21) and (22) can be combined to find the required flow numbers as a function of the downward pipe slope for balanced elongated gas pockets that are long enough to reach normal depth in the liquid film.

$$\frac{v_{sl}^2}{gD} = \frac{\sin\theta}{\lambda}\frac{D_h}{D}\left(\frac{A_n}{A}\right)^2 + \frac{A}{A_b}\frac{\cos\theta}{2\pi}\left[\frac{2}{3}\sqrt{\frac{2y_b}{R} - \left(\frac{y_b}{R}\right)^2}\left(\frac{y_b}{R} - 3\right)\left(\frac{y_b}{R} - \frac{1}{2}\right) + \arcsin\left(1 - \frac{y_b}{R}\right) + \frac{\pi}{2}\right] \tag{23}$$

These flows numbers are depicted in Figure 7 and show that the clearing velocity data, obtained by Lubbers in a 220 mm perspex pipe is matched reasonably well by the derived momentum balance.

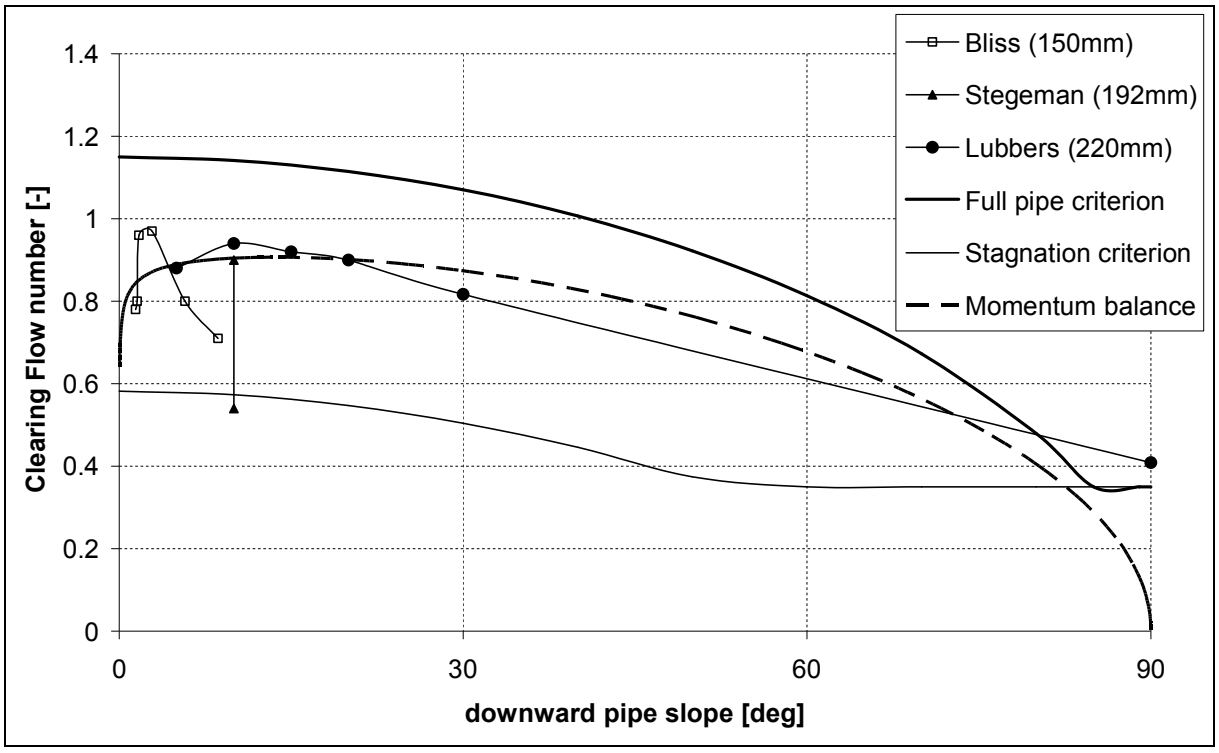

Figure 7. Clearing flow number from the momentum balance and normal flow

Another interesting feature of this momentum balance is its behaviour at very mild slopes. The flow number is zero in a horizontal pipe, but at any supercritical slope, the predicted clearing velocity is within the range obtained by the two energy criteria.

Since the momentum balance has been derived from hydrostatic pressure considerations, it is not valid anymore in a vertical pipe, in which an elongated gas pocket would break-up into smaller gas bubbles.

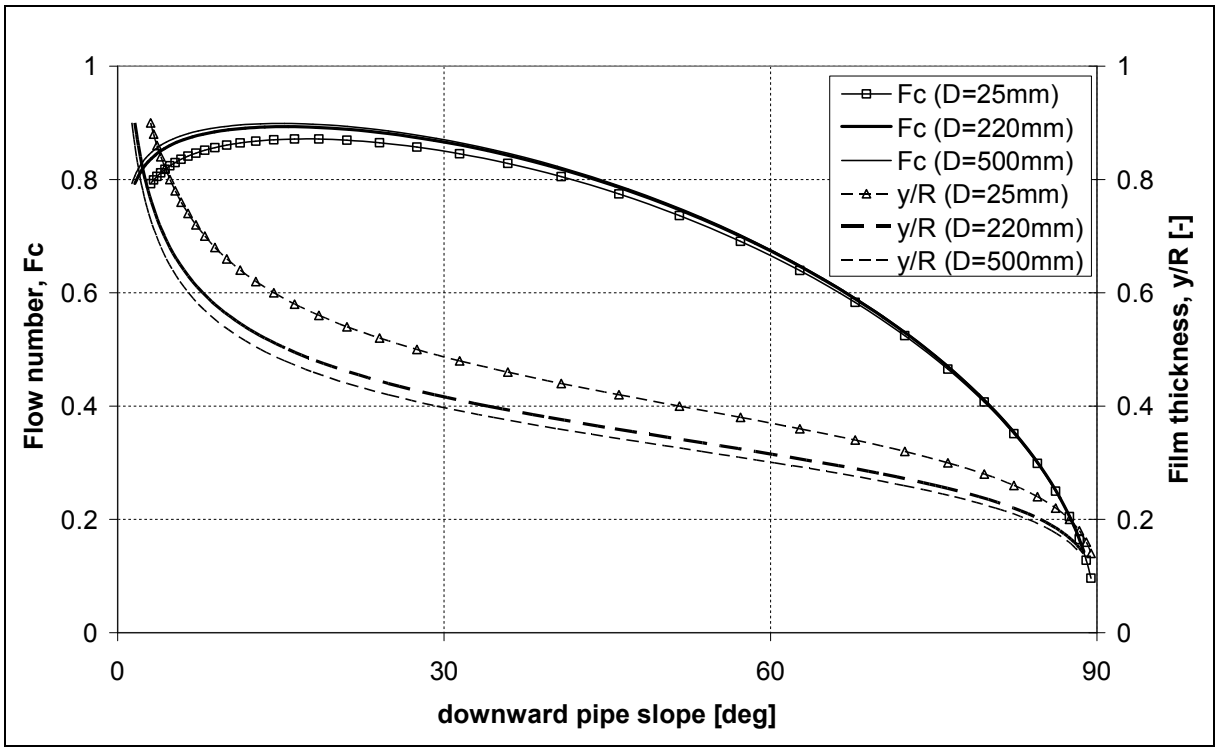

Figure 8. Sensitivity of clearing flow number for pipe diameter at a wall roughness of 0.05 mm

A numerical evaluation of equation (23) over a wide range of diameters (25 – 500 mm) and typical range of relative wall roughnesses (10^{-4} – 10^{-3}) shows that the flow number variation is less than 5% at pipe slopes greater than 5° as illustrated in Figure 8. The numerical evaluation shows that the maximum flow number of 0.90 (+0%, -3%) occurs at pipe slopes between 15° and 17°.

Kent, Gandenberger and Escarameia have measured smaller clearing flow numbers (see Figure 5). Consequently, the new momentum balance does not predict the observed reduction of the clearing flow number with pipe diameter and liquid Reynolds number. Several hypotheses can be formulated to explain this inconsistency:

1. Kent, Gandenberger and Escarameia have not evaluated sufficiently large gas pockets
2. The Reynolds influence is more pronounced than predicted by the momentum balance at pipe diameters under 200 mm.
3. Surface tension effects.

These hypotheses will be discussed separately hereafter.

One reason for this inconsistency might be the fact that Kent and Gandenberger have claimed that the clearing velocity remains constant for gas pockets with a volume greater than n = 0.5. Measurements by Lubbers on the liquid film depth show that a gas pocket in the top of a downward slope needs at least 9D to reach normal depth at downward slopes from 5° to 30°; the associated dimensionless gas volume is considerably greater than 0.5. Hence, normal depth was not reached in the experiments by Kent, Gandenberger or Escarameia. However, further inspection of Kent's and Gandenberger's datapoints shows that the clearing velocities remain constant at gas pocket volumes between n = 0.5 and n = 8.

The more pronounced Reynolds number influence at diameters under 200 mm is an unlikely reason for the smaller clearing flow numbers, if a comparison is made with Zukoski's drift velocity experiments (Zukoski 1966). The problem is that a diameter variation affects both the

Eötvös number ($Eo = \frac{\rho g D^2}{\sigma}$) for surface tension and Reynolds number ($\mathrm{Re} = \frac{v_d D}{\nu}$) for viscous effects, such that both effects cannot be studied with a single combination of fluids, like water and air. Zukoski performed drift velocity experiments with different fluids that enabled him to study the influence of the surface tension and viscous effects separately. Since the physics of drifting bubbles in upward slopes and balancing bubbles in downward slopes is very similar, it is assumed that the Reynolds number influence will be similar. Zukoski's data suggest that the drift velocity becomes independent of the Reynolds number, if the Reynolds number exceeds 200; ($\mathrm{Re} = \frac{v_d D}{\nu} > 200$); this statement is valid for all pipe angles, according to Zukoski's data. Assuming that the Reynolds influence vanishes in a similar way for balancing gas pockets, the clearing velocity should become independent of the Reynolds number for Reynolds numbers greater than 200; the Reynolds number is based on the superficial liquid velocity. Since the superficial liquid velocity is a function of the flow number and the pipe diameter, the Reynolds number criterion is expressed as follows:

$$\mathrm{Re} = \frac{v_{sl} D}{\nu_l} = \frac{F_c D \sqrt{gD}}{\nu_l} > 200 \tag{24}$$

Figure 5 shows that the minimum flow number equals 0.6, such that the criterion is satisfied for pipe diameters greater than 3.7 mm. It is concluded that Zukoski's data suggests that the Reynolds number does not explain the clearing flow number variation at pipe diameters smaller than 200 mm.

Consequently, the surface tension or Eötvös number at smaller pipe diameters, which is not included in the momentum balance derivation of equation (23), is responsible for the clearing flow number variation. A plot of the clearing flow number against the Eötvös number might support a statement on the range of applicability of the newly derived momentum balance. Since most data is available at a downward slope of 10°, Figure 9 shows the clearing flow numbers as a function of the Eötvös number. Figure 9 suggests that the clearing flow number becomes independent of the surface tension for Eötvös numbers greater than 5500 or a pipe diameter exceeding 200 mm, if the fluids are water and air. This statement is consistent with Zukoski's data on drift velocities up to Eo = 4000. Zukoski's data shows that the drift flow number depends on the Eötvös number up to Eo = 4000 for all pipe angles, except for a 90° angle (Zukoski 1966). Zukoski's drift flow numbers at 0° and 15° have been included for information in Figure 9. It is concluded from this analysis that the clearing flow number becomes independent of the surface tension at Eötvös numbers greater than 5500, although it must be noted that the empirical evidence for this statement is limited to data at a downward slope of 10°.

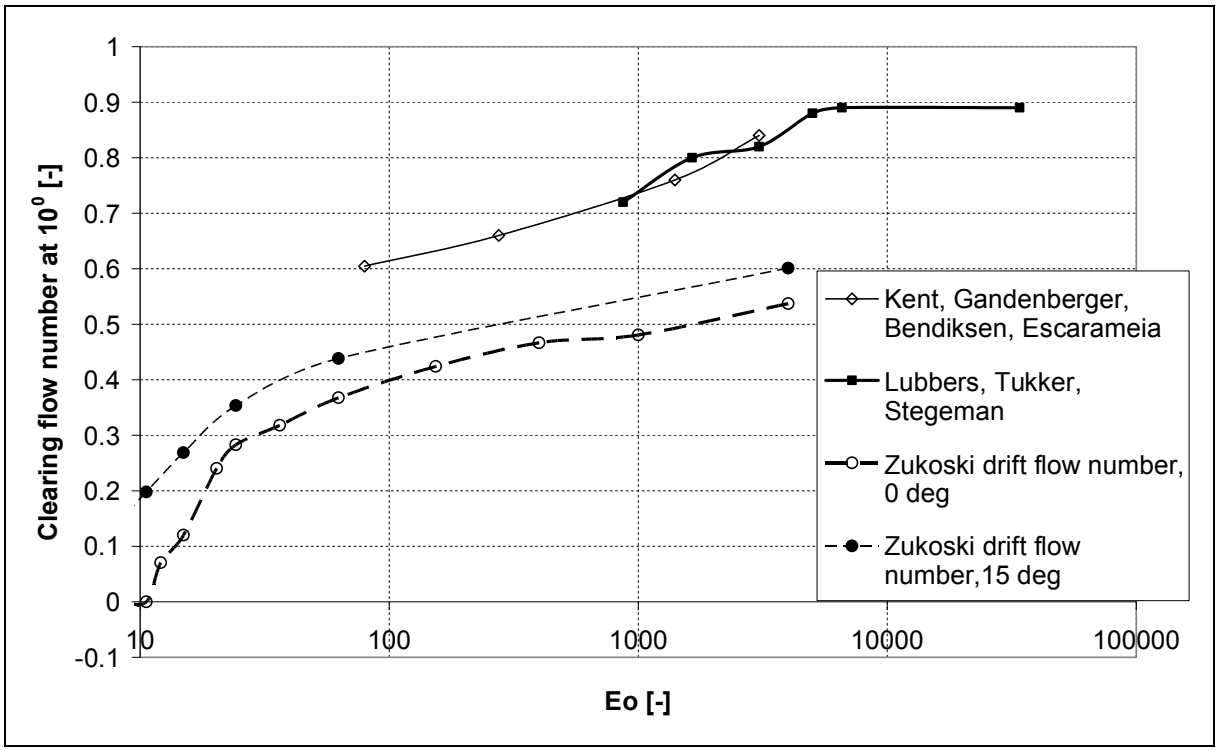

Figure 9. Clearing flow number at 10 downward slope

6. CONCLUSIONS

Two energy criteria have been derived that define the range of flow numbers within which elongated gas pockets stay balanced in a downward slope; equations (15) and (16). A new momentum-based equation has been derived that predicts the flow number or superficial liquid velocity for elongated gas pocket clearing; equation (23). This momentum balance is valid under two conditions: the liquid film velocity should reach normal depth underneath the gas pocket—this requires a gas pocket length of at least 9D; secondly the Eötvös number ($Eo = \frac{\rho g D^2}{\sigma}$) should exceed 5500, which coincides with a pipe diameter of 200 mm in a liquid-air system. If the liquid film does not reach normal depth, because of the gas pocket volume, then equation (21) can be applied to assess the clearing flow number for these smaller gas pockets. Most analytical expressions have been validated against available experimental data.

7. RECOMMENDATIONS

The empirical evidence for the minimum Eötvös number of 5500 is limited to data at a 10° downward slope. It is recommended to substantiate these findings with data at other pipe slopes and large diameter pipes.

Zukoski has found a limiting drift flow number for elongated bubbles in vertical pipes. At other angles, the drift flow number continues to increase with the Eötvös number. The maximum Eötvös number, Zukoski has tested, is 4000, for a water-air mixture in a 178 mm pipe (see Figure 9). Zukoski's dimensionless gas bubble volume was about n = 4. A similar momentum balance as derived in this paper for the clearing of gas pockets in downward

slopes can be derived for drifting gas pockets in upward slopes. The corresponding drift flow numbers are only marginally smaller than the curve for the clearing velocity, depicted in Figure 7. The momentum balance for the prediction of drift flow numbers in upward slopes could represent the limiting flow number for the elongated bubble drift velocity at arbitrary pipe slopes. This hypothesis must be verified with long elongated gas pockets in pipes greater than 178 mm diameter; the gas pockets must be long enough to enable the development of normal flow at the tail of the gas pocket, which required about 9D in downward slopes of 220mm.

The full pipe flow criterion, equation (16), has not yet been experimentally confirmed at downward pipe slopes.

ACKNOWLEDGEMENT

The authors wish to thank the participants of the CAPWAT project: Gemeentewerken Rotterdam, Waterboard Delfland, Waterboard Hollands Noorderkwartier, Waternet, Waterboard Brabantse Delta, Waterboard Reest en Wieden, Waterboard Rivierenland, Waterboard Zuiderzeeland, Waterboard Fryslân and Waterboard Hollandse Delta, Aquafin, Royal Haskoning, Grontmij Engineering Consultancy, ITT Flygt BV, Foundation Stowa and the Dutch Ministry of Economic Affairs.

NOTATION

A	Cross sectional area (m^2)	T	Interface width (m)
D	Internal pipe diameter (m)	V	Volume (m^3)
Eo	Eötvös number, defined as $Eo = \frac{\rho g D^2}{\sigma}$; also known as the Bond number (-)	v	(liquid) velocity (m/s)
F	Flow number (-)	$w(y)$	Conduit width as a function of the distance from the conduit bottom (m)
Fr	Froude number (-)	X	Liquid stagnation length (m)
g	Gravitational acceleration (m/s^2)	y	Water depth, perpendicular to pipe slope (m)
n	Dimensionless gas pocket volume, $n = V_g / (A \cdot D)$ (-)		
p	Pressure (Pa)	β	upward pipe slope (rad)
Q	Discharge (m^3/s)	θ	downward pipe slope (rad) $\theta = -\beta$
R	Pipe radius	ν	kinematic viscosity (m^2/s)
S_E	Energy slope (-)	ρ	density (kg/m^3)
		σ	surface tension (N/m)
Subscripts			
B	buoyancy	l	liquid
		n	normal (flow related)
c	clearing (velocity) i.e. for gas pocket removal	p	full pipe flow
cr	critical (free surface flow)	s	superficial or stagnation

cf	clearing velocity including friction	*w*	water
d	drift		
e	energy slope		
g	gas / air	*1*	Upstream face of control volume
h	hydraulic (radius/diameter)	*2*	Downstream face of control volume
i	incipient		

REFERENCES

Bendiksen, K., Espedal, M. (1992). "Onset of slugging in horizontal gas-liquid pipe flow." International Journal of Multiphase Flows **18**(2): 237-247.

Bendiksen, K. H. (1984). "Experimental investigation of the motion of long bubbles in inclined tubes." International Journal of Multiphase Flow **10**(4): 467-483.

Benjamin, T. B. (1968). "Gravity currents and related phenomena." J. Fluid Mech **31**: 209-248.

Bliss, P. H. (1942). The removal of air from pipelines by flowing water. J. Waldo Smith hydraulic fellowship of ASCE. Iowa, Iowa institute of hydraulic research**:** 53.

Escarameia, M. (2006). "Investigating hydraulic removal of air from water pipelines." Water Management 160(WMI): 10.

Gandenberger, W. (1957). Uber die Wirtschaftliche und betriebssichere Gestaltung von Fernwasserleitungen. Munchen, R. Oldenbourg Verlag.

Hager, W. H. (1999). "Cavity outflow from a nearly horizontal pipe." International Journal of Multiphase Flow **25**(2): 349-364.

Kalinske, A. A., Bliss, P.H. (1943). "Removal of air from pipe lines by flowing water." Proceedings of the American Society of Civil Engineers (ASCE) **13**(10): 3.

Kent (1952). The entrainment of air by water flowing in circular conduits with downgrade slope. Berkeley, California, University of Berkeley. **PhD**.

Lauchlan, C. S., Escarameia, M., May, R.W.P., Burrows, R., Gahan, C. (2005). Air in Pipelines, a literature review, HR Wallingford**:** 92.

Lubbers, C. L. (2007). On gas pockets in wastewater pressure mains and their effect on hydraulic performance. Civil engineering and Geosciences. Delft, Delft University of Technology. **PhD:** 290.

Lubbers, C. L. and F. Clemens (2005). Air and gas pockets in sewerage pressure mains. Water Science and Technology. **52:** 37-44.

Lubbers, C. L. and F. H. L. R. Clemens (2006). Breakdown of air pockets in downwardly inclined sewerage pressure mains. Water Science and Technology. **54:** 233-240.

Lubbers, C. L., Clemens, F.H.L.R. (2007). Scale effects on gas transport by hydraulic jumps in inclined pipes; comparison based on head loss and breakdown rate. 6th Int. Conference on Multiphase Flow (ICMF). Leipzig.

Montes, J. S. (1997). "Transition to a Free-surface flow at end of a horizontal conduit." Journal of Hydraulic Research **35**(2): 225-240.

Mosvell, G. (1976). Luft I utslippsledninger (Air in outfalls). Prosjektkomiteén for rensing av avløpsfann (project committe on sewage). Oslo, Norwegian Water Institute (NIVA).

Pothof, I. W. M., Clemens, F.H.L.R. (2008). On gas transport in downward slopes of sewerage mains. 11th Int. Conf. on Urban Drainage. Edinburgh.

Pothof, I. W. M., Clemens, F.H.L.R. (2009 (in review)). "On gas transport in downward slopes of sewerage mains." Water Science and Technology: 11.

Stegeman, B. (2008). Capaciteitsreductie ten gevolge van gasbellen in dalende leidingen (Capacity reduction due to gas pockets in downward sloping pipes). Civil Engineering. Zwolle, Hogeschool Windesheim. **BSc:** 62.

Taitel, Y., C. Sarica, et al. (2000). "Slug flow modeling for downward inclined pipe flow: Theoretical considerations." International Journal of Multiphase Flow **26**(5): 833-844.

Tukker, M. J. (2007). Energieverlies in dalende leidingen ten gevolge van gasbellen (head loss in downward pipes caused by gas pockets). Delft, Deltares | Delft Hydraulics**:** 48.

Wisner, P., F. N. Mohsen, et al. (1975). "REMOVAL OF AIR FROM WATER LINES BY HYDRAULIC MEANS." ASCE J Hydraul Div **101**(2): 243-257.

Zukoski, E. E. (1966). "Influence of viscosity, surface tension, and inclination angle on motion of long bubbles." Journal of Fluid Mechanics **25**(4): 821-837.